POLARIZATION OBSERVABLES OF $\vec{p}\,\vec{p} \rightarrow pp\pi^0$ NEAR THRESHOLD

P. THÖRNGREN-ENGBLOM, H.O. MEYER, J.T. BALEWSKI, J. DOSKOW, R.E. POLLOCK, B.VON PRZEWOSKI, T. RINCKEL, F. SPERISEN
Department of Physics and Indiana University Cyclotron Facility, Indiana University, Bloomington, IN 47405, U.S.A.
E-mail: meyer@iucf.indiana.edu, pia@iucf.indiana.edu

W.W. DAEHNICK, SWAPAN K. SAHA
Department of Physics, Pittsburgh University, Pittsburgh, PA 15260, U.S.A.

W. HAEBERLI, B. LORENTZ, F. RATHMANN, B. SCHWARTZ, T. WISE
Department of Physics, University of Wisconsin-Madison, Madison, WI 53706, U.S.A.

P.V. PANCELLA
Department of Physics, Western Michigan University, Kalamazoo, MI 49008, U.S.A.

With the aim to study spin dependence of pion production near threshold, an internal target facility and a forward detector have been installed in the Cooler synchrotron ring at IUCF. The detector system comprises scintillators and wire chambers. The target consists of a thin-walled open-ended storage cell into which polarized atomic hydrogen is injected. Using a stored and cooled, polarized proton beam, polarization observables of the reaction $\vec{p}\,\vec{p} \rightarrow pp\pi^0$ have been studied at energies between 21 and 55 MeV above the pion production threshold in the center of mass system. We report here measurements of the spin correlation parameters A_{xx} and A_{yy}, and the analyzing power A_y, integrated over the pion polar angle.

1 Introduction

Close to threshold for pion production in the NN system, the particles in the final state are produced in an Ss state, (the two letters denote the relative angular momentum of the two nucleons and of the pion with respect to the c.m., respectively). A measurement of σ_{tot} of $pp \rightarrow pp\pi^0$ at IUCF at bombarding energies between 285 and 325 MeV [1], exceeded by a factor of five the theoretical predictions at the time, which were based on direct production and on-shell rescattering mechanisms [2]. The energy dependence is well described by phase space and the final state interaction between the two protons in an effective-range approximation [1]. In order to account for the magnitude of the total cross section additional effects from the exchange of the σ and ω mesons were incorporated into the calculations and thus it was considered that there was evidence for heavy meson exchange in the short-range NN interaction [3, 4]. Inclusion of the off-shell rescattering amplitude was also shown to account for the discrepancy between experiment and theory [6]. Among the most recent theoretical work is a comprehensive model calculation also taking into account explicitly the role of the Δ isobar [5]. Attempts to explain the Ss partial wave strength in the framework of chiral perturbation have met with little success, so far [7]. The interpretation of the data remains inconclusive whereas the experimental results were confirmed and also extended closer to threshold by an experiment at CELSIUS for beam energies between 281 and 310 MeV [8].

As the proton bombarding energy is raised, the contributions of partial waves with a Ps or Pp final state become important. In order to separate these contributions and thus discriminate between different production mechanisms and models, polarization observables are required. In this experiment, we have measured the spin-dependent cross section $\Delta\sigma_T$, the spin correlation parameters A_{xx} and A_{yy}, and the analyzing power A_y in a study of $\vec{p}\vec{p} \to pp\pi^0$ at beam energies 325, 350, 375 and 400 MeV. In section 2 the experiment is described. The data analysis and the results are presented in section 3. The conclusion and further plans are summarized in section 4.

2 The Experiment

2.1 Beam and Target

The proton beam was stack-injected into the Cooler synchrotron ring at IUCF with filling rates of 30-100 μA/min. After filling for 2-3 minutes acceleration to the bombarding energy of choice was done. Data were taken during the flattop which lasted typically 5-8 minutes, after which the remaining beam was discarded. The beam lifetime was of the order of 0.5 to 1 h. The cooled proton beam is characterized by its very good energy resolution $\delta p/p$ of the order of 10^{-5} and its exceptionally small emittance of 0.1 π mm mrad [12].

The target was a polarized atomic hydrogen gas storage cell installed in the A-region of the Cooler, fed by an atomic beam source [9]. At this location of the ring the β functions are small ($\beta_x = 0.9$ m and $\beta_y = 1.7$ m) and the dispersion is practically zero. This means that the target cell diameter can be small which helps to achieve a thicker target and thus sufficient luminosity to measure polarization observables for total cross sections on the order of tens of μb. The cell is a 12 mm diameter cylinder constructed from 25 μm thick Teflon-coated aluminum foil. The Teflon surface preserves the polarization during the approximately 300 wall collisions that the hydrogen atoms undergo. The atomic beam is injected through a second 11 mm diameter tube with a wall thickness of 75 μm that is spot-welded to and intersects the storage cell at

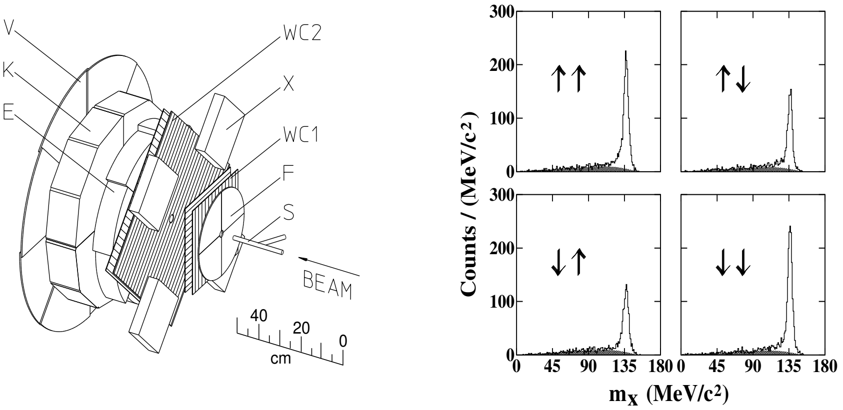

Figure 1: (left) Forward detector and storage target cell, letters as explained in the text. (right) Spinsorted distributions of the calculated missing mass (m_x) at T_{beam} = 325 MeV. The arrows indicate parallell or antiparallell beam and target polarization. The shaded area is the assumed background.

30° to the normal. For background and systematic error studies unpolarized gas can be fed into center of the cell through a small spot-welded fitting on the 11 mm tube. Mounted outside of the target chamber are three magnetic guide field coils that govern the polarization direction of the target. The operational field strength was 0.2 - 2.0 mT, chosen such as to minimize the perturbations of the closed orbit of the beam. Change of guide field direction is done every 2 s and does not affect the magnitude of polarization [10]. The time constant of the polarization reversal is 7 ± 1 ms [11] and data taking is off for 100 ms during every reversal. Beam polarization was vertical (±y) and the target polarization was switched between vertical (±y) and horizontal (±x). Thus a total of 8 spin combinations were used.

2.2 Forward detector

Particles emanating from near threshold reactions are peaked in the forward direction in the laboratory system and thus a large acceptance can be achieved with a relatively modest sized detector. For measuring the four-momentum of the two outgoing protons from $\vec{p}\vec{p} \to pp\pi^0$ four scintillator planes and two wire chambers have been mounted within one meter downstream of the storage target cell (S), cf. Fig. 1. The maximum θ_{lab} of the protons ranges from 22 to 33 degrees for bombarding energies in the interval 325 to 400 MeV. This angular range is fully covered except at 400 MeV where there is a cut-off at the utmost angles. The detectors are mounted symmetrically surrounding the beampipe which set the limit of the minimum detection angle to $\theta_{lab} \simeq 5°$.

The four scintillator planes, with thicknesses of 1.5 mm (F), 103 mm (E), 153 mm (K) and 6.4 mm (V), are all made of Bicron (BC408) and segmented into four (F, K) or eight sectors (E, V). The outer radii are 203 mm (F), 369 mm (E), 423 mm (K) and 610 mm (V). The position dependence of the light collection efficiency is obtained from the data and is used to determine the absolute proton energies on an event-by-event basis.

For monitoring of luminosity and the beam and target polarization pp elastic scattering is detected in four additional scintillators (X) placed at $\theta_{lab} = 45°$ at four azimuthal angles $\phi = \pm 45°$ and $\phi = \pm 135°$. The thickness of these detectors is 51 mm. The product of beam and target polarization ($\mathrm{P_B} \cdot \mathrm{P_T}$) is obtained by measuring the spin correlation coefficient combination $A_{xx} - A_{yy}$ which is large at $\theta_{lab} = 45$ degrees [13]. The integrated luminosity $\int Ldt$ is given by the known pp elastic cross section.

Track reconstruction is based on information from the two wire chambers, each with two orthogonal planes. The wire spacings are 3.175 mm and 6.35 mm, respectively. To avoid ambiguities where 2 prong events hit the same wire the chambers are rotated 45° with respect to each other. The speciality of the design is that at the center of the sensitive area there is an opening that allows for the beam pipe to come through [14].

The trigger for an event to be processed in the data acquisition as a 2 prong event is that one or more F-segments and at least two E-segments fire but the V-plane does not. For diagnostics and detector tests single prongs are also recorded. The overlap between neighboring scintillator segments, designed to avoid dead areas, is taken into account in the matching between the particle's reconstructed track and which scintillator sectors that fired.

3 Data analysis and Results

For the primary event selection the following cuts and conditions are imposed to the data: Particle identification is done by means of time-of-flight(E-F) vs. the energy deposited in the E-detector (for protons that are stopped in the E-detector) or by ΔE/E plots, i.e. E vs. K (for protons passing through the E-detector). A cut is done in the reconstructed vertex spectrum of the event, which shows the extended target of the storage cell. An angular 2D cut is made for the opening angle between the two protons vs. their difference in ϕ. The four wire chamber signatures that are processed are the 2222, 2221, 2223, 2233 multiplicities, where each number denotes the number of clusters in the four planes (ideally always two). The parameters of two straight lines passing through a common origin on the beam axis is fitted in an iterative process to the input wire positions, and a cut is made in the spectrum of the χ^2 of the adopted best fit.

3.1 Energy calibration

The light (corrected for position dependence) collected in the stopping scintillators E and K are added together. The resolution of the π^0 missing mass peak determines the multiplicative constant of an assumed linear calibration (the effect of a second degree correction is negligible for the observables studied), and the offset is decided such that the unpolarized θ distribution of the π^0 in the c.m. system is symmetric. The constants are correlated and thus determined simultaneously.

3.2 Systematic errors

The effects on the observables by varying the event selection criteria were studied in a systematic way. The results obtained for reasonable variations were all within statistical errors and were averaged over in the final result.

One non-negligible effect was the error originating from the amount of background subtraction. It was estimated by varying the integration limits of the π^0 peak, and added in quadrature to the statistical error. Particles that go undetected into the beam pipe represent a potential systematic error. The final-state interaction between the two protons is only prominent in a relative S-wave and thus a bias is introduced in the ratio to the other partial waves. In the analysis the $\Delta\sigma_T$ was studied as a function of an artificial θ_{lab} cut-off using an effective-range expansion for the pp final-state interaction [1]. A fit was made and extrapolated to 0°. The correction was the size of an error bar. The effect from the hole on the other observables was found to be negligible.

3.3 Results

The missing-mass spectrum of the undetected π^0 was sorted according to beam and target spin combinations in order to determine $\Delta\sigma_T$, defined as the difference of the two cross sections $\sigma(\uparrow\downarrow + \downarrow\uparrow\ ) - \sigma(\uparrow\uparrow - \downarrow\downarrow)$, where the arrows denote $\pm y$ polarization of beam and target, respectively, cf. Fig. 1.

The spin dependent cross section (see Appendix A of Ref. [16]) can, for the non-zero beam and target polarization components in the present experiment, be written as

$$\sigma(\overline{P}^B, \overline{P}^T) = \sigma_0[1 + (P_y^B A_y^B + P_y^T A_y^T)\cos\phi - P_x^T A_y^T \sin\phi$$
$$+P_y^B P_x^T \frac{A_{xx} - A_{yy}}{2} \sin 2\phi + P_y^B P_y^T (\frac{A_{xx} + A_{yy}}{2} - \frac{A_{xx} - A_{yy}}{2} \cos 2\phi)]. \quad (1)$$

where σ_0 is the unpolarized cross section, ϕ is the azimuthal angle of the π^0, $P_{x(y)}^{B(T)}$ denote the horizontal (vertical) polarization of beam (target) and $A_y^{B(T)}$ is the angle-integrated analyzing power related to the beam (target). For $\vec{p}\,\vec{p} \to pp\pi^0$ we have $A_y^B \equiv -A_y^T$.

The expected ϕ dependencies were fitted to the spin-sorted experimental ϕ_{π^0} distributions corresponding to the analyzing power A_y and the spin correlation coefficient combinations $A_{xx} - A_{yy}$ and $A_{xx} + A_{yy}$, (the latter identical to $-\Delta\sigma_T/\sigma_{tot}$). The results for the spin observables are given in Ref. [15] and shown in Fig. 2. Also depicted are curves according predictions by a microscopic model calculation made by C. Hanhart et al., which is based on direct production and off-shell rescattering. Contributions from HME (ω) are added and the Δ isobar is included explicitly [5, 17].

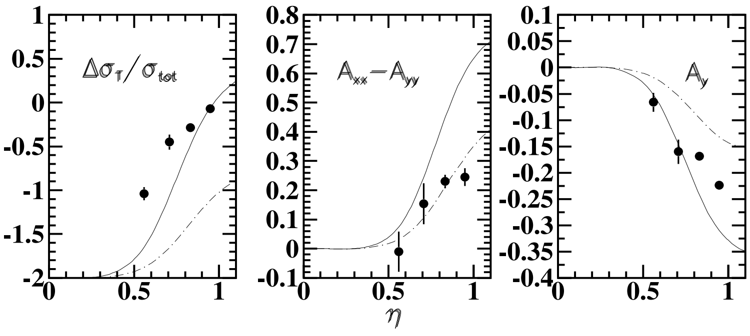

Figure 2: The observables $\Delta\sigma_T/\sigma_{tot}$, $A_{xx} - A_{yy}$ and A_y as a function of η, the maximum momentum of the pion in the c.m. system divided by m_π. The full-drawn line represents the full model as described in the text, the dashed-dotted line is calculated excluding the Δ.

4 Conclusion

We have described an experimental set-up and the first useful measurements of spin observables of pion production below a bombarding energy of 400 MeV. Theoretical predictions for these observables are still scarce and at variance with our data [5]. Recent new activity in the field will presumably lead to further understanding of the production mechanisms for near threshold pion production. In progress with the same set-up are also measurements with a polarized beam with both y- and z-components in combination with a target polarized in x-, y- and z-directions. Thus we will be able to determine $\Delta\sigma_L$, A_{xz} and A_{zz} and finally to deduce in a model-independent way the contributions of individual partial waves in this energy domain.

References

1. H.O. Meyer et al., *Nucl. Phys.* A **539**, 633 (1992)
2. D.S. Koltun and A. Reitan, *Phys. Rev.* **141**, 1413 (1966)
3. T.-S. Lee and D. Riska, *Phys. Rev. Lett.* **70**, 2237 (1993)
4. C.J. Horowitz, H.O. Meyer and D.K. Griegel, *Phys. Rev.* C **49**, 1337 (1994)
5. C. Hanhart et al., FZ Jülich preprint, nucl-th/9808020
6. E. Hernandez and E. Oset, *Phys. Lett.* B **350**, 158 (1995)
7. T. Sato et al., *Phys. Rev.* C **56**, 1246 (1997)
8. A. Bondar et al., *Phys. Lett.* B **356**, 8 (1995)
9. T. Wise, A.D. Roberts and W. Haeberli, *Nucl. Inst. Meth.* A **336**, 410 (1993)
10. W. Haeberli et al., *Phys. Rev.* C **55**, 597 (1997)
11. F. Rathmann et al., *Phys. Rev.* C **58**, 658 (1998)
12. R.E. Pollock and P. Schwandt, *IUCF Newsletter* **43**, 3-7 (3 Oct 1988)
13. B. von Przewoski et al., *Phys. Rev* C **58**, 1897 (1998)
14. K. Solberg et al., *Nucl. Inst. Meth.* A **281**, 283 (1989)
15. H.O. Meyer et al., *Phys. Rev. Lett.* **81**, 3096 (1998)
16. H.O. Meyer, *Phys. Rev.* C **56**, 2074 (1997)
17. C. Hanhart, private communication